Toxicology xxx (xxxx) 153695

Contents lists available at ScienceDirect

Toxicology

journal homepage: www.elsevier.com/locate/toxicol

Endoplasmic reticulum stress and pro-inflammatory responses induced by phthalate metabolites monoethylhexyl phthalate and monobutyl phthalate in 1.1B4 pancreatic beta cells

Fulya Dal Yöntem [a, b], Sinem Ayaz [c, d], Şeyma Bulut [e, f], Ebru Haciosmanoğlu Aldoğan [g], Müfide Aydoğan Ahbab [h, *]

[a] Koç University, Faculty of Medicine, Department of Biophysics, Istanbul, Turkey
[b] Koç University Research Center for Translational Medicine (KUTTAM), Istanbul, Turkey
[c] Istanbul University, Cerrahpasa, Institute of Graduate Studies, Department of Clinical Microbiology, Istanbul, Turkey
[d] Haliç University, Faculty of Medicine, Department of Clinical Microbiology, Istanbul, Turkey
[e] Bezmialem Vakif University, Faculty of Medicine, Department of Medical Biology, Istanbul, Turkey
[f] Bezmialem Vakıf University, Institute of Health Sciences, Department of Biotechnology, Istanbul, Turkey
[g] Bezmialem Vakif University, Faculty of Medicine, Department of Biophysics, Istanbul, Turkey
[h] University of Health Sciences Türkiye, Hamidiye Vocational School of Health Services, Istanbul, Turkey

ARTICLE INFO

Handling Editor: Dr. Mathieu Vinken

Keywords:
Phthalates
1.1B4 Pancreatic beta cells
Monoethylhexyl phthalate
Monobutyl phthalate
Diabetes
ER stress

ABSTRACT

In recent years, phthalates and their metabolites have been associated with metabolic diseases such as diabetes mellitus. To investigate the effects of phthalate metabolites exposure on insulin production and release, 1.1B4 pancreatic beta cells were treated with different concentrations (0.001–1000 μM) of monoethylhexyl phthalate (MEHP) and monobutyl phthalate (MBP). For such purpose, the 1.1B4 cells were evaluated for their viability, apoptosis rate, lysosomal membrane permeabilization (LMP), mitochondrial membrane potential (ΔΨm), oxidative stress, ER stress status, in addition to their secretory functions. MEHP, not MBP, exhibited a notable reduction in metabolic viability, particularly at higher concentrations (500 and 1000 μM) following 24-hour exposure. Similarly, both MEHP and MBP induced decreased metabolic viability at high concentrations after 48- and 72-hour exposure. Notably, neither MEHP nor MBP demonstrated a significant impact on apoptosis rates after 24-hour exposure, and MBP induced mild necrosis at 1000 μM concentration. Cell proliferation rates, indicated by PCNA expression, decreased with 10 and 1000 μM MEHP and 0.1 and 10 μM MBP exposures. LMP analysis revealed an increase in 1000 μM MBP group. Exposure to 0.001 μM of both MEHP and MBP significantly reduced cellular glutathione (GSH) levels. No significant change in intracellular reactive oxygen species (ROS) levels and ΔΨm was observed, but MBP-exposed cells exhibited elevated levels of lipid peroxidation. Functional assessments of pancreatic beta cells unveiled reduced insulin secretion at low glucose concentrations following exposure to both MEHP and MBP, with concurrent alterations in the expression levels of key proteins associated with beta cell function, including GLUT1, GCK, PDX1, and MafA. Moreover, MEHP and MBP exposures were associated with alterations in ER stress-related pathways, including JNK, GADD153, and NF-κB expression, as well as PPARα and PPARγ levels. In conclusion, this study provides comprehensive insights into the diverse impacts of MEHP and MBP on 1.1B4 pancreatic beta cells, emphasizing their potential role in modulating cell survival, metabolic function, and stress response pathways.

Abbreviations: **ATF4,**, Activating transcription factor 4; **JNK,**, c-Jun N-terminal kinase; **DBP,**, Dibutyl phthalate; **DEHP,**, Diethylhexyl phthalate; **ER,**, Endoplasmic reticulum; **GCK,**, Glucokinase; **GLUT1,**, Glucose transporter 1; **GSH,**, Glutathione; **GADD153,**, Growth arrest- and DNA damage-inducible gene 153; **CHOP,**, also known as; **LMP,**, Lysosomal membrane permeabilization; **MafA,**, MAF bZIP transcription factor A; **MDA,**, Malondialdehyde; **MBP,**, Monobutyl phthalate; **MEHP,**, Monoethylhexyl phthalate; **(NF-κβ,**;, Nuclear factor kappa B; **PDX1,**, Pancreatic duodenal homeobox 1; **PPAR,**, Peroxisome proliferated-activated receptor; **PCNA,**, Proliferating cell nuclear antigen; **ROS,**, Reactive oxygen species; **PERK,**, Protein kinase RNA-like endoplasmic reticulum kinase

* Correspondence to: Hamidiye Vocational School of Health Services, University of Health Sciences Türkiye, Üsküdar, Istanbul, Turkey.
E-mail addresses: mufideaydogan@gmail.com, mufideaydogan.ahbab@sbu.edu.tr (M.A. Ahbab).

https://doi.org/10.1016/j.tox.2023.153695
Received 6 October 2023; Received in revised form 25 November 2023; Accepted 30 November 2023
0300-483/© 20XX

CORRECTED PROOF

Note: Low-resolution images were used to create this PDF. The original images will be used in the final composition.

1. Introduction

Diabetes mellitus (DM) has been identified as a group of metabolic diseases characterized by high blood glucose levels (hyperglycemia) resulting from defects in insulin secretion, insulin action, or both (ADA, 2014). The prevalence of diabetes has increased globally over the two decades (ADA, 2020). With various genetic and environmental factors, hyperglycemia can be caused by the progressive destruction and/or dysfunction of insulin secreting pancreatic β cells (IDF, 2021). Therefore, any chemical with a potential to damage these cells and alter their hormonal function can lead the onset and development of diabetes (Deng et al., 2018).

Phthalates are chemicals that are widely used as plasticizers and additives in the production of plastic materials to make them more flexible (Latini, 2005; Net et al., 2015). Due to their non-covalent bond to plastic, phthalates are gradually distributed to different environmental compartments (Latini, 2005; Nam et al., 2020) and have been found in closed environments, consumer foods, human urine, milk and amniotic fluid (Del Bubba et al., 2018; Hammel et al., 2019; Bräuner et al., 2022; Mok et al., 2022).

Recent in vitro, in vivo, and epidemiologic studies have suggested a relationship between phthalate exposure and diabetes (Mangala Priya et al., 2014; Dong et al., 2017; Li et al., 2019; Venturelli et al., 2019; Shi et al., 2020). When exposed to humans through various routes, phthalates are typically metabolized to their metabolites (Wang et al., 2019). Diethylhexyl phthalate (DEHP) metabolites and monobutyl phthalate (MBP) have been associated with elevated fasting blood glucose in cross-sectional epidemiologic studies (James-Todd et al., 2016; Saengkaew et al., 2017; Dales et al., 2018). In vivo exposure to DEHP has been associated with high plasma glucose and low insulin levels (Martinelli et al., 2006; Rajesh et al., 2013). Rats exposed to high doses of DEHP and DBP during gestation and lactation showed increased fasting blood glucose in adulthood, along with abnormal beta cell structure and reduced pancreatic insulin content (Lin et al., 2011; Venturelli et al., 2019). Furthermore, DEHP exposure is associated with decreased insulin secretion, while DEHP metabolites are associated with elevated fasting insulin levels and impaired beta cell function (Huang et al., 2014; Zhang et al., 2017a; Dales et al., 2018). Elevated DBP levels may decrease insulin secretion and exacerbate type 2 diabetes mellitus (T2DM) by disrupting the insulin signaling pathway and impairing insulin secretion (Deng et al., 2018).

A study of diabetic patients found a positive association between urinary phthalate metabolite concentrations and urinary malondialdehyde (MDA) levels, an oxidative stress biomarker (Duan et al., 2017). Furthermore, a direct link has been established between the production of reactive oxygen species (ROS) and cellular mechanisms such as protein oxidation and protein folding (Bhandary et al., 2013). Misfolded proteins can induce protein aggregation by inducing endoplasmic reticulum (ER) stress, a factor that contributes to the pathophysiology of conformational diseases such as neurodegenerative disorders and diabetes mellitus. ER stress results from the disruption of homeostasis and accumulation of unfolded and misfolded proinsulin in the ER lumen and induces β cell dysfunction that plays an important role in T2DM (Fonseca et al., 2011). Several proteins and pathways have been implicated in the regulation of ER stress and the unfolded protein response, such as inositol-requiring kinase 1 (IRE1), pancreatic ER eIF2α kinase (PERK), and activating transcription factor 6 (ATF6) (Cao and Kaufman, 2014). CHOP/GADD153 (growth arrest/DNA damage) is primarily associated with the unfolded protein response and has been identified as a major mediator of ER stress-induced apoptosis (Sano and Reed, 2013). The deleterious effect of DEHP on INS-1 cells, which are lines derived from a rat insulinoma, has been documented through the induction of apoptosis due to the activation of the PERK/ATF4/CHOP ER stress signaling pathway coupled with the suppression of antioxidant defense mechanisms (Sun et al., 2015).

When examining the in vitro effects of DEHP and DBP, it is more accurate to focus on the effects of MEHP and MBP as they rapidly convert into their metabolites upon entering the body (Moreau et al., 2022). In this study, it was investigated whether exposure to MEHP and MBP at human-relevant concentrations (0.001–1000 μM) affects 1.1B4 pancreatic beta cell function by examining ROS and lipid peroxidation production and antioxidant status, cellular insulin secretion and content, and ER stress activation.

2. Material and Methods

2.1. Chemicals

MAF bZIP transcription factor A (MafA) (Cat. No. sc-390491), glucokinase (GCK) (Cat. No. sc-17819), pancreatic duodenal homeobox 1 (PDX1) (Cat. No. sc-390792), proliferating cell nuclear antigen (PCNA) (Cat. No. sc-7907), glucose transporter 1 (GLUT1) (Cat. No. sc-377228), growth arrest- and DNA damage-inducible gene 153 (GADD153, also known as CHOP) (Cat. No. sc-7351), c-Jun N-terminal kinase (JNK) (Cat. No. sc-7345), PPARγ (Cat. No. sc7273), and PPARα (Cat. No. sc-398394) antibodies and N-Acetyl-L-cysteine (NAC) (Cat. No. sc-202232) were purchased from Santa Cruz Biotechnology (Texas, USA). β-actin (Cat. No. CST, #3700 and nuclear factor kappa B (NF-κB) (Cat. No. D14E12) antibodies were purchased from Cell Signaling Technology. MEHP (Cat. No. ALR-138N; purity of 98.9%) and MBP (Cat. No. ALR-135N; purity of 97.4%) were purchased from AccuStandard (New Haven, CT).

2.2. Cell culture and exposures

1.1B4 (human pancreatic beta cells) were purchased from European Collection of Authenticated Cell Cultures (ECACC) and grown in RPMI 1640 containing 10% (v/v) fetal bovine serum at 37 °C in a 5% CO_2 incubator. Experiments conducted through the use of secondary cell culture. 1.1B4 cells were utilized within passages 10–15 to ensure reproducibility and maintain characteristic phenotypic features. The cells were seeded to reach 70–80% confluence before treatment. 1.1B4 cells were treated with various concentrations (0–1000 μM) of MEHP or MBP for 24 h. Both phthalates were dissolved in dimethyl sulfoxide (DMSO, Sigma) with the final concentration of 0.1% of DMSO in the cell culture medium. 1.1B4 cells were also treated with 2.5 μM NAC. The MEHP and MBP concentrations used in this study covers concentrations above and below those reported for human exposure (Morgenstern et al., 2017; Sakhi et al., 2017; Li et al., 2022; Liu et al., 2022; Peng et al., 2023).

2.3. Cell viability assay

Cell viability was determined using the 3-(4, 5-dimethylthiazol-2-yl) − 2, 5-diphenyltetrazolium bromide (MTT) (98%, Alfa Aesar) reagent. Briefly cells were seeded into 96 well plates at a density of 1×10^4 cells/well and were cultured with absence or presence of various concentrations (0.001–1000 μM) of MEHP or MBP for 24, 48 and 72 h. After exposures cells were incubated with 0.1 mg/mL MTT reagent for 2 h. Cell culture medium was removed and 100 μL DMSO was added onto each well as stopping solution. Absorbance was measured at 570 nm using an automated microplate reader (Thermo Scientific, Multiskan GO). Brightfield images were taken by using Zeiss Axiovert 5 microscope.

2.4. Western blot analysis

1.1B4 cells were cultured with absence or presence of various concentrations (0.001–1000 μM) of MEHP or MBP for 24 h were harvested and lyzed by radioimmunoprecipitation (RIPA) assay buffer (San-

CORRECTED PROOF

taCruz) according to the manufacturer's instructions. The protein content was quantified using Bradford Assay. Similar amounts of total protein were resolved by SDS-PAGE and transferred onto a polyvinylidene difluoride (PVDF) membrane (Life Technologies, CA, USA). The membrane was blocked with 5% bovine serum albumin (BSA) in a tris-buffered saline with Tween-20 (TBS-T) for 1 h at room temperature and then incubated with primary antibodies [β-actin (1:1000), GADD153 (1:200), PCNA (1:200), PPARα (1:1000), PPARγ (1:1000), PDX-1 (1:500), JNK (1:500), MafA (1:500), GCK (1:1000), GLUT1 (1:1000), NF-κβ (1:1000)] overnight at 4 °C. The appropriate horseradish peroxidase conjugated secondary antibodies (1:3000) were used to detect primary antibodies, and enzymatic signals were visualized by were visualized by chemiluminescent detection with enhanced chemiluminescence (ECL) substrate (ThermoScientific). Protein bands were analyzed by using Image J software (Stael et al., 2022).

2.5. Mitochondrial membrane potential (ΔΨm) measurements

The mitochondrial membrane potential ($\Delta\Psi_m$) of 1.1B4 cells cultured with absence or presence of various concentrations (0.001–1000 μM) of MEHP or MBP for 24 h were measured by flow cytometry (BD Accuri C6, Becton Dickinson) using Rhodamine 123 (Rho123, ThermoScientific). Briefly cells were incubated with 1 μg/mL Rhodamin 123 at 37 ^{0}C 5% CO_2 for 15 min. After incubation cells were washed with cold PBS twice. 500 μL cold PBS were added onto cells. A minimum of 20,000 gated events were collected on flow cytometer for each sample and membrane potentials were analyzed compared to control cells.

2.6. Intracellular ROS production assay

1.1B4 cells (2×10^5 cells) cultured with absence or presence of various concentrations (0.001–1000 μM) of MEHP or MBP for 24 h were stained for 30 min at 37 °C with 10 μM 2′,7′-dichlorodihydrofluorescein diacetate (DCFDA; Sigma) then washed and analyzed by flow cytometry. A minimum of 20,000 gated events were collected on flow cytometer for each sample.

2.7. MDA assay

1.1B4 cells (2×10^5 cells) treated with various concentrations of MEHP or MBP (0–1000 μM) for 24 h. After exposure, lipid peroxidation was measured as the level of MDA determined by the thiobarbituric acid (TBA) reaction following the manufacturer's instructions (TBARS Assay Kit; Biorbyt, Cambridge, UK) (Armstrong and Browne, 1994). The absorbance was measured at 535 nm. The concentration of MDA is expressed as mM of MDA/mg of protein.

2.8. Lysosomal membrane permeabilization (LMP) assay

1.1B4 cells were seeded onto 6 well plates at a density of 2×10^5 cells and treated with various concentrations of (0–1000 μM) MEHP and MBP for 24 h. After exposure cells were washed with 1x PBS once and stained with 2 μg/mL acridine orange (Sigma) for 20 min at 37 °C. LMP was assessed both by fluorescent microscopy imaging by using inverted fluorescent microscope (Zeiss, Axio Observer Z1) and flow cytometric analyzes. Acridine orange passively diffuses membranes and accumulated in acidic lysosomal lumen with a red fluorescence. During lysosomal leakage, cytosolic acid levels rise (Wang et al., 2018). At elevated LMP, leakage of acridine orange accumulated in the lysosome into the cytosol causes a concomitant increase in green cytosolic staining and a decrease in red lysosomal staining (Eriksson et al., 2023).

2.9. Apoptosis assay

Apoptotic and necrotic cells were determined by using Annexin V-FITC/Propidium Iodide apoptosis kit according to the manufacturer's instructions (BD Biosciences Pharmingen Co., USA). Briefly MEHP and MBP treated 1.1B4 cells were washed with cold PBS (1x) twice and then 1×10^6 cells/mL were suspended in 1x binding buffer. Stained cells were acquired by using BD Accuri C6 Flow Cytometer and data were analyzed by using BD Accuri C6 Plus software.

2.10. Insulin assay

1.1B4 cells were seeded onto 6 well plates at a density of 3×10^5 cells and treated with MEHP and MBP for 24 h. After exposure, cells were incubated in Krebs-Ringer bicarbonate (KRB) buffer (pH 7.4) supplemented with 10 mM/l HEPES and 1.1 mM glucose at 37 °C for 1 h. Then the cells were supplemented with KRB-HEPES buffer with 1.1 mM glucose (fasting glucose conditions) or 16.7 mM glucose (high glucose conditions) for 1 h. The supernatant was collected for insulin release. The cells were lyzed with acid/ethanol with rigorous pipetting. The samples were centrifuged, and the supernatant was stored for analysis of insulin content. The samples were stored at − 80 °C. The insulin release and contents were analyzed with an ELISA kit (Mercodia, AB, Sweden). Protein contents of the samples were determined with Bradford Assay to normalize the insulin content of the cells.

2.11. Total glutathione (GSH) assay

GSH assay was performed with using Glutathione Assay Kit (Sigma). 1.1B4 cells were seeded at a density of 3×10^5 cells and treated with MEHP and MBP for 24 h. After exposure, the cells were harvested with and scrapers with PBS. The samples were centrifuged at 700 g for 5 min and then the cell pellets were washed in ice cold 1x PBS. The cell pellets were incubated with iced cold assay buffer for 10 min and then added 5% 5-Sulfosalicylic acid solution was added. The samples were centrifuged at 10000 g for 10 min at 4 °C. The supernatant was analyzed for total GSH with according to kit protocols and the results were normalized to protein content.

2.12. Statistical analysis

All experimental data are shown as mean ± standard deviation (SD). Analysis was performed using GraphPad Prism 8 (GraphPad Software, San Diego, CA, USA). Significant differences among groups were determined using one-way ANOVA followed by the Bonferroni post hoc test for multiple comparisons or multiple t-test. The level of $p < 0.05$ was considered to indicate a statistically significant difference.

3. Results

3.1. MEHP but not MBP reduces metabolic viability and proliferation in human pancreatic beta cells at high concentrations

MTT is a cell viability assay based on metabolic activity of the cells that uses the ability of cells to reduce MTT reagent to a colored reporter, formazan crystals. After exposure 1.1B4 cells with various concentrations (0–1000 μM) of MEHP and MBP for 24-, 48- and 72-hours metabolic viability was evaluated by using MTT assay (Fig. 1A). It was noted that MEHP, but not MBP, decreased cell metabolic viability at high concentrations (500 and 1000 μM) after 24 h exposure ($p < 0.0001$ and $p = 0.0001$, respectively). After 48 h the metabolic viability of the 1.1B4 cells was decreased to 33.67% and 84.06% at 500 μM ($p < 0.0001$ and $p = 0.004$, respectively) and 8.71% and 75.69% at 1000 μM ($p < 0.0001$ and $p = 0.002$, respectively) MEHP and MBP exposures, respectively, compared to control. 72 h exposure

CORRECTED PROOF

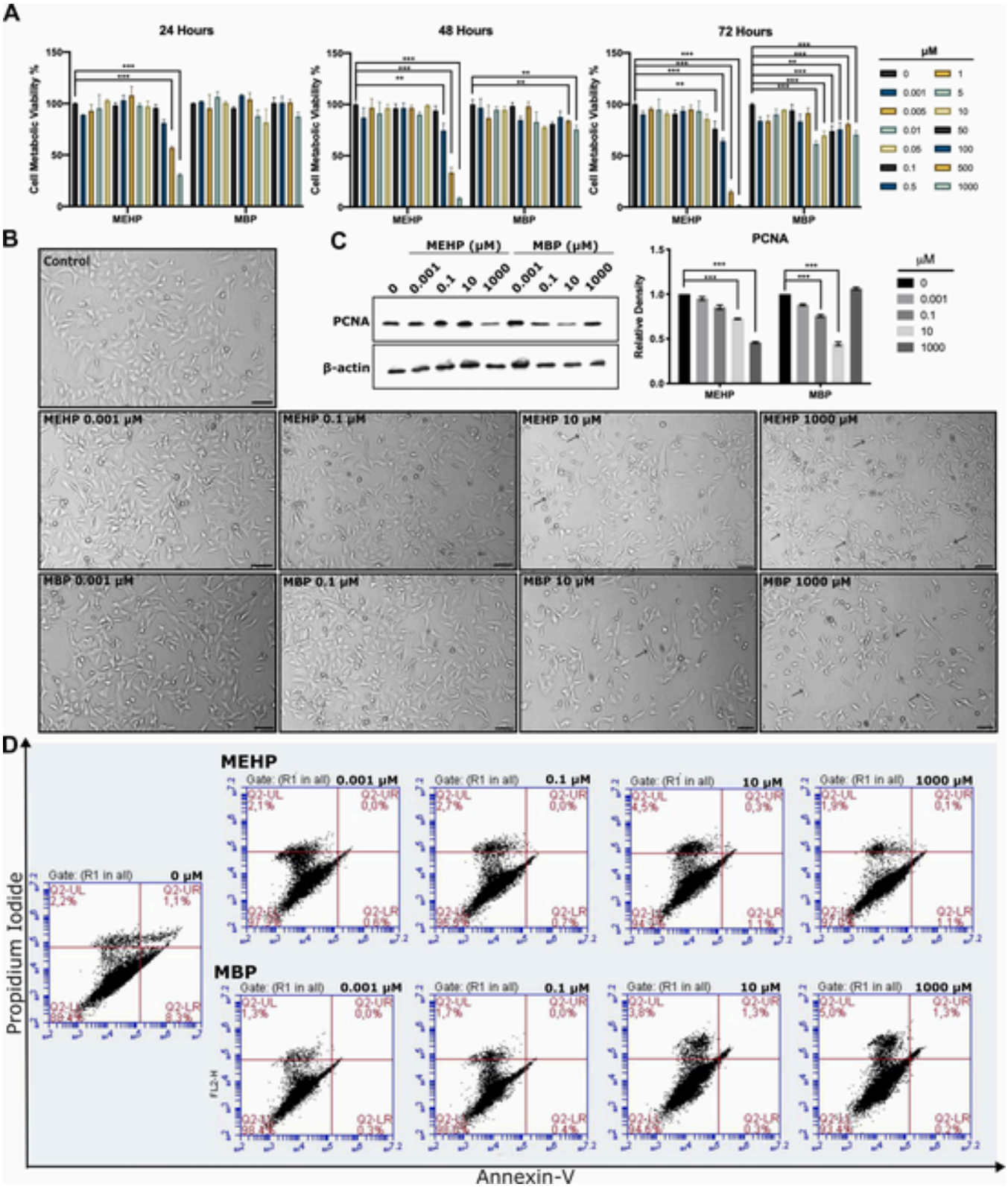


Fig. 1. Effects of MEHP and MBP on 1.1B4 cell metabolic viability, proliferation and cell death pathways. (A) Metabolic viability of 1.1B4 cells cultured in the absence or presence of various concentrations (0.001–1000 μM) of MEHP and MBP for 24, 48 and 72 h. The data are expressed as percentages of untreated control cells.). * *p < 0.01; * **p < 0.001; compared with untreated control cells, according to one-way ANOVA. **(B)** Morphology analysis of 1.1B4 cells cultured in the absence or presence of various concentrations (0.001–1000 μM) of MEHP and MBP for 24 h, 4x magnification, scale bars: 10 μm. Arrows indicate the formation of elongated cells observed in 10 and 1000 μM MEHP and MBP treated cells. Brightfield images were taken by using Zeiss Axiovert 5 microscope. **(C)** PCNA western blot bands and relative protein expression density bar graph of 1.1B4 cells cultured in the absence or presence of various concentrations (0.001–1000 μM) of MEHP and

Fig. 1.—*continued*
MBP for 24 h. β-actin was used as the loading control. Band intensities were normalized to corresponding β-actin intensity. * **p < 0.001; compared with untreated control cells, according to multiple t-test. **(D)** Apoptosis/necrosis assay analysis of 1.1B4 cells cultured in the absence or presence of various concentrations (0.001–1000 μM) of MEHP and MBP for 24 h. Annexin-/PI- represents live cells, Annexin-/PI+ represents necrotic cells, Annexin + /PI+ represents late apoptotic cells and Annexin + /PI- represents early apoptotic cells. Columns show mean values of three independent experiments (± SD).

of 1.1B4 cells to MEHP and MBP resulted in decreased cell metabolic viability at 1000 μM, 1.88% and 70.49%, ($p < 0.0001$ and $p = 0.0002$, respectively) compared to control. Moreover, both MEHP and MBP exposures caused to shift the structure of the cells to a more elongated form as the concentrations increased (Fig. 1B). When it was evaluated whether decrease of cell metabolic viability was associated with apoptosis at MEHP or MBP treated cells, there was no significant difference at early/late apoptotic of MEHP and MBP treated cells compared to control group (Fig. 1D). It was clearly seen with brightfield microscopy images that cell confluency was decreased in MEHP and MBP exposed groups however there was no induction of apoptosis. With increasing concentration, exposure to MBP induced very mild necrosis, but not apoptosis, in 1.1B4 cells. When cell proliferation rates were evaluated by PCNA protein expression, 10 and 1000 μM MEHP ($p < 0.0001$) and 0.1 and 10 μM MBP ($p < 0.0001$, for both) exposures decreased PCNA protein expression levels compared to control cells (Fig. 1C).

3.2. MBP induces LMP of human pancreatic beta cells

LMP is one of the mechanisms involved in cell death and it is initiated in the early phase of apoptosis (Boya and Kroemer, 2008). In order to determine whether MEHP or MBP exposure induced LMP, acridine orange-stained cells were imaged by fluorescence microscopy and analyzed by flow cytometry. As indicated by cytosolic acidification, the fluorescence microscopy results revealed that LMP was increased with increasing concentrations in MBP-treated cells, however there was no change in MEHP exposure at any concentration used (Fig. 2A). In flow cytometric analysis, LMP increased in the 1000 μM MBP group ($p = 0.0006$) as evidenced by decreased red fluorescence intensity of 1.1B4 cells stained with acridine orange (Fig. 2B).

3.3. Low concentrations of MEHP and MBP reduces GSH levels

GSH levels in the cell determines the cellular redox potential and thus regulates the modulation of apoptosis (Hall, 1999). 1.1B4 cells were treated with various concentrations of (0–1000 μM) MEHP and MBP for 24 h and total GSH levels was assessed. 0.001 μM of MEHP and MBP significantly decreased GSH% of the cells to 39% and 54%, respectively ($p = 0.03$ for both) (Fig. 3A). Interestingly as the concentrations increased total GSH% were recovered as high as 83% for 10 μM MEHP and 80% for 0.1 μM MBP exposure. There was no change in intracellular ROS levels of 1.1B4 cells treated with MEHP and MBP for 24 h when compared to control group (Fig. 3B). Between the control and MEHP/MBP exposure groups, there was no change in mitochondrial membrane potential (Fig. 3C). MDA levels can be measured by means of TBARS for the analysis of lipid peroxidation (Katerji et al., 2019). After 24 h of exposure MDA levels were increased up to 2.55-fold in MBP-treated 1.1B4 cells ($p < 0.0001$), but not in MEHP-treated cells compared to control (Fig. 3D).

3.4. Pancreatic beta cell functions after MEHP and MBP exposure

The insulin ELISA results revealed that at low glucose concentrations (1.1 mM) 0.001 and 10 μM MEHP treated cells insulin secretion decreased to 0 and 0.04 μIU/μg protein when compared to control cells ($p = 0.005$), 0.07 μIU/μg protein (Fig. 4A), after 24 h exposure. 0.001 and 10 μM MBP exposure also decreased insulin secretion of 1.1B4 cells at low glucose concentrations to 0.037 and 0.027 μIU/μg protein, respectively, however there was no change at insulin content at any exposure group after 24 h exposure (Fig. 4A-B). MEHP exposure did not demonstrate any noteworthy variation in secretion in comparison to control cells at high glucose concentrations of 16.7 mM. Furthermore, insulin secretion was not detected in the MBP group (Fig. 4C). At high glucose concentrations (16.7 mM), insulin content decreased significantly to 3.96 μIU/μg protein at 0.001 μM MEHP treated cells compared to control cells insulin content 6.77 μIU/μg protein ($p = 0.005$) (Fig. 4D). There was no significant change at insulin content of other exposure groups. To find out whether pancreatic beta cell function related protein change after MEHP and MBP exposures, GLUT1, GCK, PDX1 and MafA expression levels were analyzed. Exposure to MEHP resulted in a significant two-fold decrease in GLUT1 expression levels ($p = 0.0006$). Conversely, GCK expression levels increased at lower MEHP concentrations (0.001 and 0.1 μM) ($p = 0.0005$ and $p = 0.0002$) but decreased at 1000 μM ($p = 0.006$) (Fig. 4E-F). PDX-1 expression levels increased at 0.001 and 10 μM MEHP ($p = 0.004$), and MafA expression levels increased at all MEHP exposures except decreased at 1000 μM ($p < 0.0001$). Similarly, 0.1, 10, and 1000 μM MBP exposures significantly increased GLUT1 expression ($p = 0.0004$, $p = 0.0004$, and $p = 0.0001$, respectively), with a two-fold increase observed at 1000 μM MBP. No significant changes in GCK expression were noted with MBP

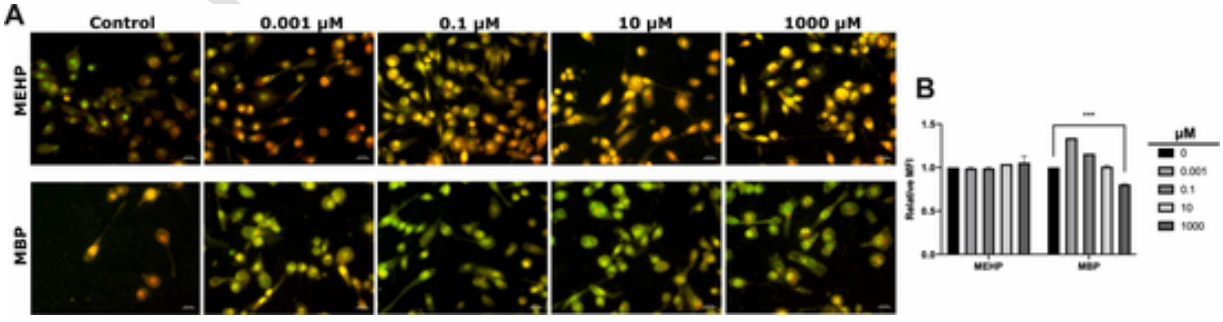


Fig. 2. Effects of MEHP and MBP on LMP (A) Acridine orange staining of 1.1B4 cells cultured in the absence or presence of various concentrations (0.001–1000 μM) of MEHP and MBP for 24 h. The images were captured by inverted fluorescent microscope (Zeiss, Axio Observer Z1). Scale bars: 0.2 mm. **(B)** Mean fluorescence intensity (FL2) of acridine orange-stained 1.1B4 cells cultured in the absence or presence of various concentrations (0.001–1000 μM) of MEHP and MBP for 24 h. Acridine orange, which accumulates in the lysosome and emits red fluorescence, leaks into the cytosol with an increase in LMP, resulting in an increase in green fluorescence. The decreased red fluorescence and increased green fluorescence of acridine orange indicate increased LMP, which may indicate high cytoplasmic acidification. Columns show mean values of three independent experiments (± SD). * ** p = 0.0006 compared with untreated control cells, according to multiple t-test.

RECORD PROOF

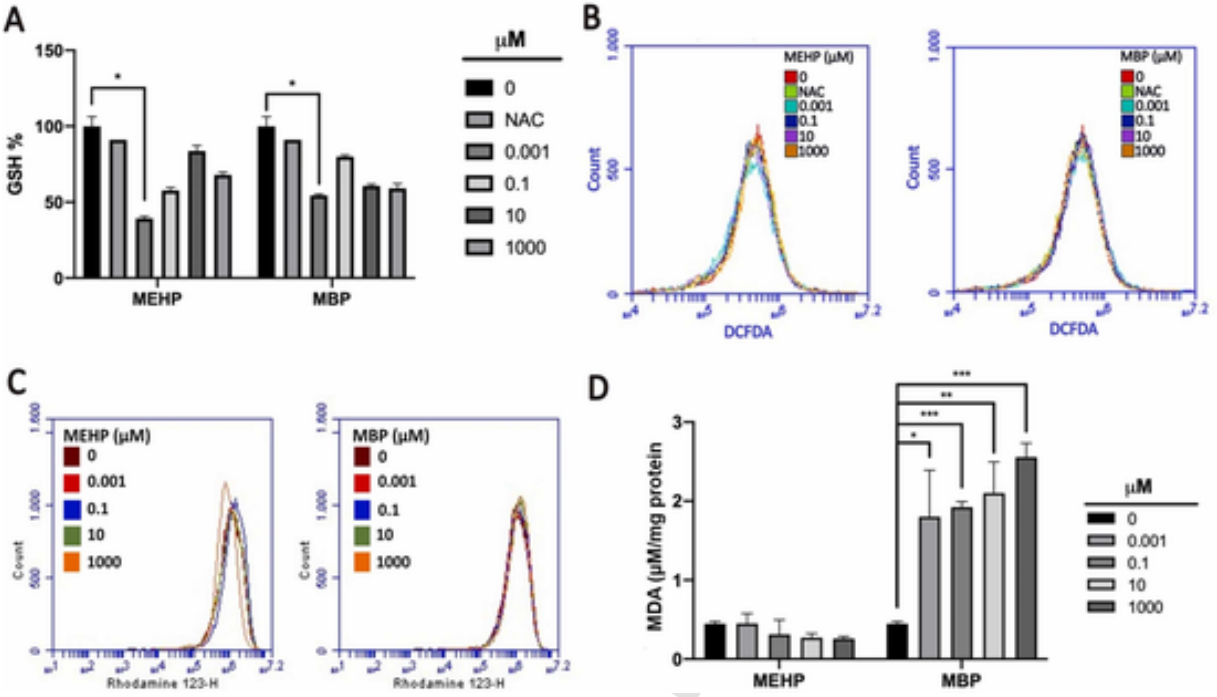


Fig. 3. Redox and metabolic impacts of MEHP and MBP exposure in 1.1B4 cells. (A) GSH levels of 1.1B4 cells cultured in the absence or presence of various concentrations (0.001–1000 μM) of MEHP and MBP for 24 h **(B)** Total ROS levels of 1.1B4 cells cultured in the absence or presence of various concentrations (0.001–1000 μM) of MEHP and MBP for 24 h and were determined by flow cytometric analyses using DCFDA staining were **(C)** ΔΨm of 1.1B4 cells cultured in the absence or presence of various concentrations (0.001–1000 μM) of MEHP and MBP for 24 h and were determined by flow cytometric analyses using Rhodamine 123 staining. **(D)** MDA levels in 1.1B4 cells cultured in the absence or presence of various concentrations (0.001–1000 μM) of MEHP and MBP for 24 h. Columns show mean values of three independent experiments (± SD). *p < 0.05; * *p < 0.01; * **p < 0.001; compared with untreated control cells, according to multiple t-test.

exposure. PDX-1 expression levels increased at 0.1, 10, and 1000 μM MBP ($p = 0.012$, $p = 0.049$, and $p = 0.0003$, respectively), while MafA expression levels increased at all MBP exposures, including a 6-fold increase at 1000 μM ($p < 0.0001$) (Fig. 4E-F).

3.5. ER stress related protein levels after MEHP and MBP exposure

GADD153 expression levels were increased in all exposure groups of MEHP and MBP compared to control group, except for 1000 μM MEHP-treated cells ($p < 0.0001$) (Fig. 5A/B). JNK expression levels were also decreased with 0.1, 10 and 1000 μM MEHP ($p = 0.0003$ and $p = 0.001$, respectively for 10 and 1000 μM) and 0.001 and 0.1 μM MBP exposure ($p = 0.015$ and $p = 0.001$ respectively). There was no significant difference in JNK expression of other exposure groups compared to control group. Although NF-κB expression levels decreased at a concentration of 1000 μM MEHP exposure ($p = 0.0003$) and increased at 0.001 and 0.1 μM MEHP exposure ($p = 0.012$ and $p = 0.006$, respectively), there is a concentration-dependent increase of NF-κB expression levels in MBP-exposed cells compared to the control group (Fig. 5B). In 1000 μM MBP treated cells, NF-κβ expression levels increased almost by 2-fold ($p = 0.0001$). The expression levels of PPARα and PPARγ exhibited a concentration-dependent decrease in all MEHP exposure groups, except for PPARγ levels in the low-concentration (0.001 μM) group ($p = 0.003$) (Fig. 6). Conversely, within the MBP exposure group, PPARα protein levels decreased in all concentration except for 1000 mM concentration group. Furthermore, exposure to 0.001, 0.1, and 1000 μM MBP led to a reduction in PPARγ protein levels ($p = 0.0004$, $p = 0.003$ and $p = 0.0001$ respectively) (Fig. 6).

4. Discussion

This study presents in-depth findings on the varied effects of MEHP and MBP exposure at human-relevant concentrations on 1.1B4 pancreatic beta cells, highlighting their potential involvement in regulating cell viability, metabolic function, and stress responses. MEHP and MBP decreased cells metabolic viability in a concentration- (0.001–1000 μM) and time-dependent (24, 48, 72 h) manner. These low concentrations (0.001, 0.005, 0.01, 0.05, 0.05, 0.1, 0.5 μM) of MEHP and MBP found to have no significant effect on metabolic viability while high concentration of MEHP and MBP inhibited 1.1B4 cell metabolic viability, especially after 48- or 72-hours exposure. Exposure to MEHP and MBP may cause a decrease in the cell proliferation rate of 1.1B4 cells. This suggests that these compounds primarily affect cell survival rather than inducing cell death. This is inferred from decreased levels of PCNA protein, which is associated with cell division. Furthermore, the absence of apoptosis or necrosis after MEHP exposure suggests that the decrease in proliferation is due to a slowdown in cell division and not cell death. Conversely, MBP exposure caused mild necrosis but no apoptosis in 1.1B4 cells as the concentration increased. Furthermore, LMP increased in cells treated with high concentration of MBP but remained unchanged by MEHP exposure. Lysosomes are membrane-enclosed cytoplasmic organelles that control the intracellular turnover of macromolecules and contain many different types of hydrolytic enzymes (Boya and Kroemer, 2008). LMP is a pathway that regulates cell death under physiological conditions and contributes to cell death in many pathological situations, including necrotic cell death (Serrano-Puebla and Boya, 2016). Several synthetic and endogenous substances have been identified as triggers of LMP, eliciting a wide range of effects on membrane trafficking, energy metabolism, and cell viability (Boya and Kroemer, 2008). For instance, exposure to 200 μM MEHP was demonstrated to activate autophagic flux, leading to LMP in EA.hy 926 cells (Wu et al., 2017). Similarly, INS-1 cells treated with 0–400 μM DEHP for 1 h increased LMP (She et al., 2017). In contrast to this study, both studies were performed with cells of different origin (rat insulinoma cell line INS-1 and human endothelial cell EA.hy 926) or the parent chemical DEHP. Massive lysosomal degradation can lead to cytoso-

CORRECTED

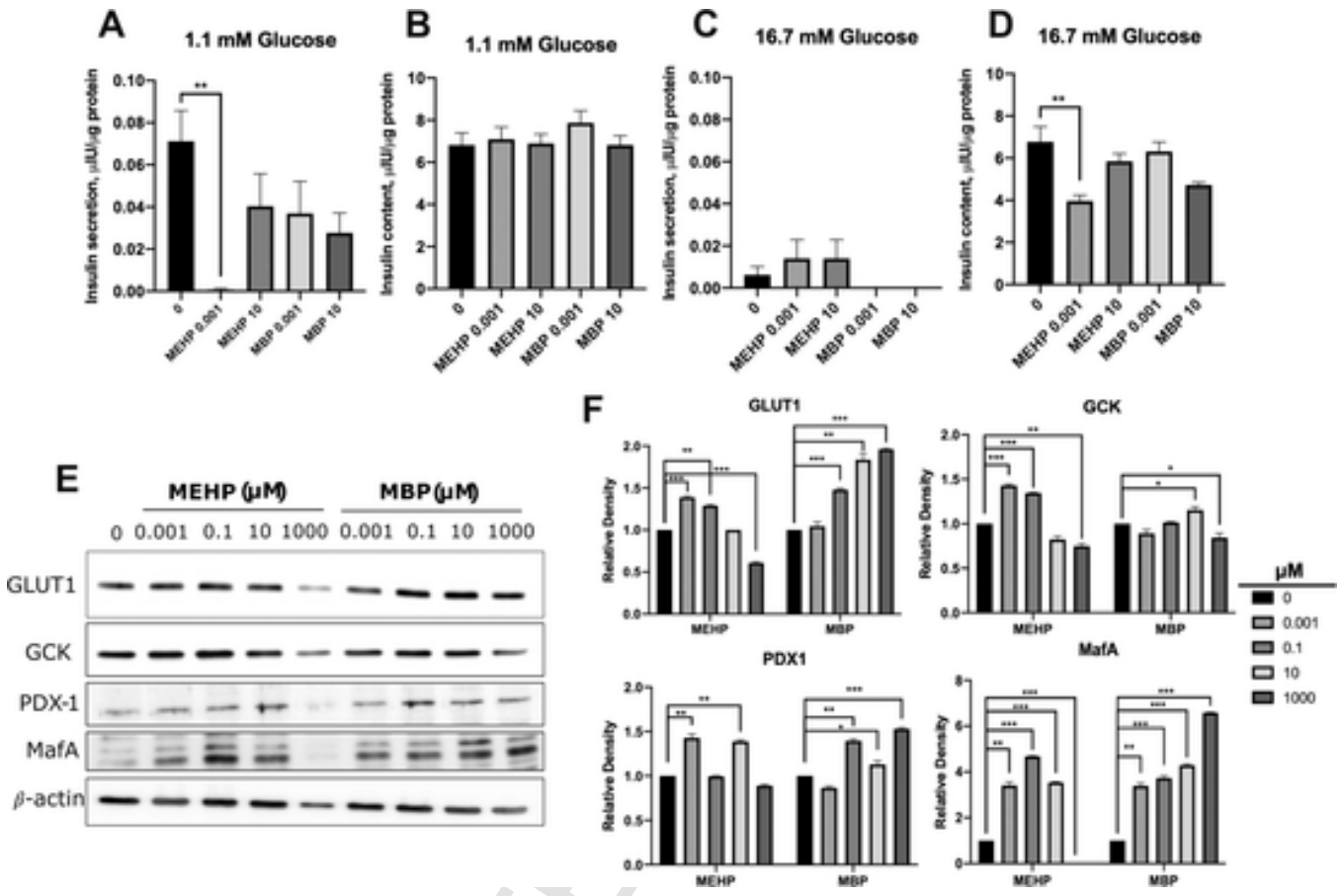


Fig. 4. MEHP and MBP Exposure Suppresses Insulin Secretion and Regulates Pancreatic Beta Cell Function-Related Proteins (GLUT1, GCK, PDX1, MafA) in 1.1B4 Cells. 1.1B4 cells cultured in the absence or presence of various concentrations (0.001–1000 µM) of MEHP and MBP for 24 h. Insulin secretion **(A)** and content **(B)** after 1.1 mM glucose. Insulin secretion **(C)** and content **(D)** after 16.7 mM glucose. * *p < 0.01 compared with untreated control cells, according to one-way ANOVA. (E) Representative western blot bands of GCK, GLUT1, PDX-1, MafA and β-actin and (F) relative protein expression density bar graph of 1.1B4 cells cultured in the absence or presence of various concentrations (0.001–1000 µM) of MEHP and MBP for 24 h. β-actin was used as the loading control. Band intensities were normalized to corresponding β-actin intensity. β-actin was used as the loading control. Band intensities were normalized to corresponding β-actin intensity. Columns show mean values of three independent experiments (± SD). *p < 0.05; * *p < 0.01; * **p < 0.001; compared with untreated control cells, according to multiple t-test.

lic acidification, which in turn can cause cell death by necrosis (Boya and Kroemer, 2008). In this study, the mild necrosis after exposure of 1.1B4 cells to MBP may have resulted from increased cytosolic acidification as shown by LMP analysis by fluorescence microscopy.

The results of the study show that the 1.1B4 cells exhibit different reactions to MEHP and MBP in terms of oxidative stress. Oxidative stress can be caused by exogenous oxidants and compounds that promote the formation of ROS or compromise antioxidant defense mechanisms (Lushchak, 2014). The current study revealed no changes in ROS levels or ΔΨm in 1.1B4 cells treated with MEHP and MBP for 24 h in comparison to control in contrary of previous studies with DEHP or MEHP (She et al., 2017; Wu et al., 2017; Shi et al., 2020). Elevated levels of intracellular ROS resulted in mitochondrial dysfunction, including impaired mitochondrial activity and loss of ΔΨm (Lu and Gong, 2009). ROS have short-lifespan and show rapid reactivity with components that regulate the redox state. Therefore, oxidative stress is assessed by examining the oxidative damage caused by these radicals to the lipids, proteins and nucleic acids of cells (Katerji et al., 2019). MDA, a widely studied end product of lipid peroxidation, serves as a reliable indicator for ROS-mediated damage to cell membranes. In this study, it is particularly noteworthy that MBP-treated 1.1B4 cells had elevated MDA levels after 24 h, in contrast to MEHP-treated cells. Moreover, lower concentrations of MEHP and MBP considerably reduce the GSH level in 1.1B4 cells, but the total GSH percentage recuperates promptly at higher concentrations that indicate additional evidence of GSH's susceptibility to chemical exposure. GSH is the most abundant non-enzymatic antioxidant and plays a critical role in metabolic protective functions such as hydroperoxide reduction, free radical scavenging and xenobiotic detoxification (Wu et al., 2004). MEHP reduced GSH levels in INS-1 cells based on concentration-dependency (Shi et al., 2020). In summary, this study reveals unique reactions to MEHP and MBP concerning oxidative stress, ΔΨm, and GSH regulation in 1.1B4 cells.

In order to investigate the interaction between phthalate metabolites and beta cell function objectively, we examined insulin release and cell contents of 1.1B4 cells under exposure to MEHP and MBP at fasting and high glucose conditions. Previous studies suggest that phthalate exposures may impair insulin secretion, but these studies observed insulin secretion only in high dose administration groups (Sun et al., 2015; Weldingh et al., 2017; Karabulut and Barlas, 2021). In contrast, this study found that exposure to low concentrations of MEHP (0.001 µM) resulted in a decrease in insulin secretion under fasting glucose conditions. Moreover, 0.001 µM MEHP exposure group also exhibited a decrease in insulin content during high glucose conditions compared to the control. Insulin secretion decreased in MBP-treated 1.1B4 cells but, similar to other studies, no statistically significant difference was observed (Weldingh et al., 2017). These results implicate that MEHP exposure, especially low concentrations, may cause disruption of insulin production and secretion, possibly due to impaired glucose sensing or

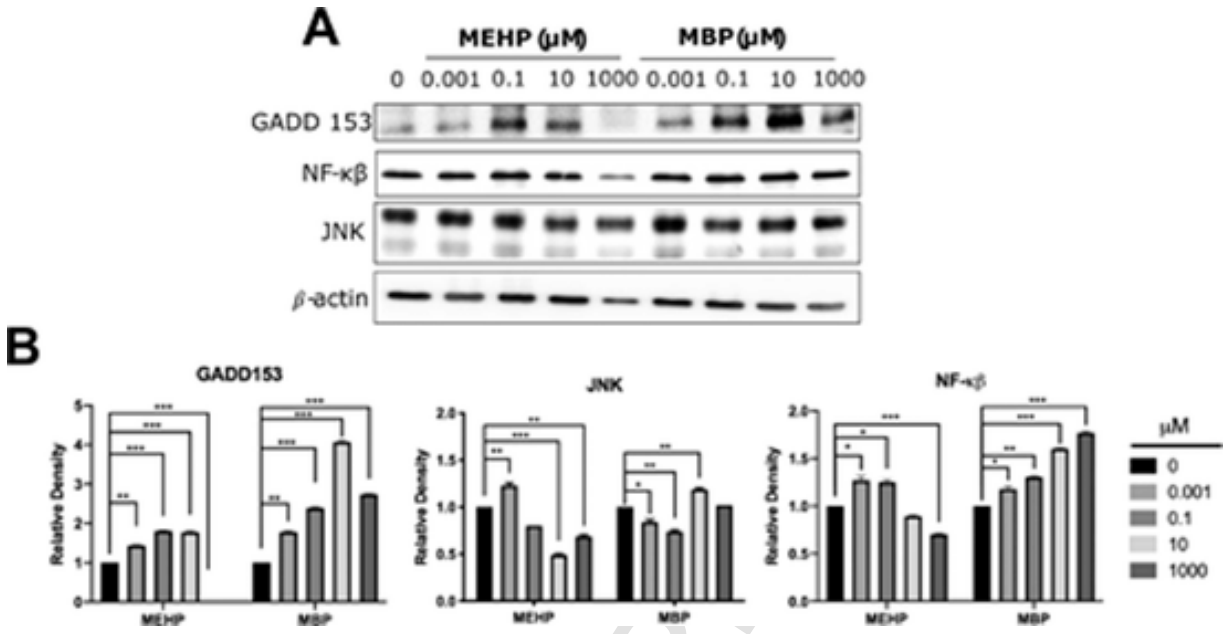


Fig. 5. MEHP and MBP Exposure Induces Prominent Alterations in ER Stress and Inflammatory Markers GADD153, JNK, and NF-κB in 1.1B4 Cells. (A) Representative western blot bands of GADD153, NF-κβ, JNK and β-actin and **(B)** relative protein expression density bar graph of 1.1B4 cells cultured in the absence or presence of various concentrations (0.001–1000 μM) of MEHP and MBP for 24 h. β-actin was used as the loading control. Band intensities were normalized to corresponding β-actin intensity. Columns show mean values of three independent experiments (± SD). *p < 0.05; * *p < 0.01; * **p < 0.001; compared with untreated control cells, according to multiple t-test.

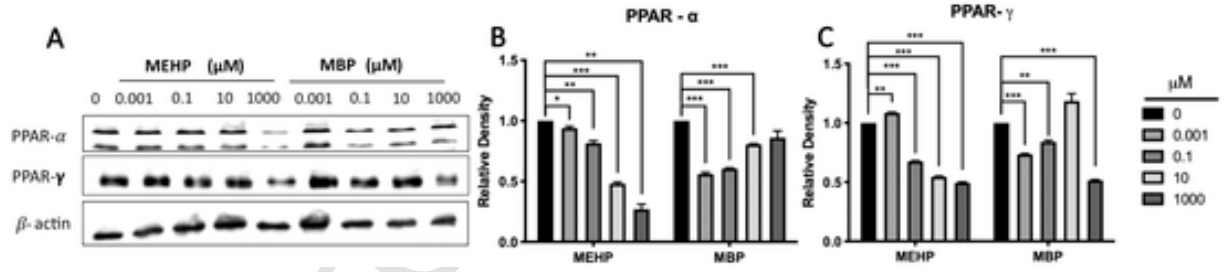


Fig. 6. MEHP Exposure Predominantly Suppresses PPARα and PPARγ Expression, while MBP Shows Concentration-Specific Effects in 1.1B4 Cells. (A) Representative western blot bands of PPARα, PPARγ and β-actin and **(B)** relative protein expression density bar graph of 1.1B4 cells cultured in the absence or presence of various concentrations (0.001–1000 μM) of MEHP and MBP for 24 h. β-actin was used as the loading control. Band intensities were normalized to corresponding β-actin intensity. Columns show mean values of three independent experiments (± SD). *p < 0.05; * *p < 0.01; * **p < 0.001; compared with untreated control cells, according to multiple t-test.

signaling pathways within the beta cells (Cerf, 2013). Therefore, in this study, protein levels of GLUT1, GCK, PDX-1 and MafA, key proteins associated with pancreatic beta cell function, were determined to provide a deeper understanding of the molecular mechanisms underlying the observed dynamics of insulin secretion. Glucose is the main energy source for various tissues in the body and carried into the pancreatic β-cells via GLUT1 in humans and GLUT2 in rodents (McCulloch et al., 2011) and 1.1B4 cells are shown to express GLUT1 (McCluskey et al., 2011). GLUT1 and GCK protein levels elevated in 1.1B4 cells treated with low concentration of MEHP in comparison to the control, while they decreased in the cells treated with high concentration of MEHP. This study shows that exposure with low concentrations of MEHP can lead to upregulation of these proteins, possibly to promote glucose uptake and metabolism. This suggests that 1.1B4 cells may initiate a defense mechanism to counteract low concentration of MEHP toxicity. Conversely, both GLUT1 and GCK protein levels decreased in cells treated with high concentrations of MEHP. GCK is a pivotal enzyme in glucose metabolism, especially within pancreatic β-cells, where it functions as a glucose sensor and essential regulator of glucose-stimulated insulin secretion (Wang and Iynedjian, 1997). This decrease at higher MEHP concentrations indicates a possible dose-dependent effect on these proteins. Furthermore, these results suggest that low and high doses of MEHP exposure may affect these protein levels by different mechanisms. Unlike MEHP, MBP-treated cells showed a significant increase in GLUT1 expression levels, with the most pronounced 2-fold increase observed in cells exposed to high concentrations of MBP. Furthermore, GLUT1 protein levels of 1.1B4 cells increased after 24 and 72 h MEP exposures in our previous study with monoethyl phthalate (Güven et al., 2016). Consistent with this finding, a reduction in insulin secretion was observed in 1.1B4 cells following exposure to 0.001 and 10 μM MBP. These observations suggest a potential interaction between increased GLUT1 expression and altered insulin secretion dynamics in response to MBP exposure.

PDX1 is a transcription factor that plays a central role in the function and survival of beta cells in the pancreas (Fujimoto and Polonsky, 2009). PDX-1 expression significantly increased in cells treated with 0.001 and 10 μM MEHP and 0.1, 10 and 1000 μM MBP compared to the control group. Likewise, MafA expression increased 3-fold with all exposures except for a decrease observed in the high concentration of MEHP group. Remarkably, all MBP exposures resulted in a significant

increase in MafA expression, with a striking 6-fold increase observed at high concentration of MBP and more than a threefold increase at other concentrations. At the transcriptomic level, the abundance of β-cells characterized by elevated PDX1 and MafA expression disrupts gene pathways integral to metabolic processes (Nasteska et al., 2021). Intriguingly, MafA and PDX1 overexpression throughout the islet has been linked to disturbances in Ca^{2+} flux and insulin secretion, a phenomenon mirrored in the decreased insulin secretion observed within the exposure groups with elevated PDX1 and MafA. MafA activity is high under healthy islet conditions, but it has been shown to increase as a protective mechanism against acute oxidative stress (Kitamura et al., 2005). MafA controls numerous β-cell-specific genes, including insulin, GLUT2 and PDX1 (Wang et al., 2007). Interestingly, a study involving INS-1 cells demonstrated that cordycepin could enhance the expression of GLUT1 mRNA and protein, as well as PDX1 (Sun et al., 2022), suggesting a link between the elevated protein levels of MafA and PDX1 and the increased protein expression of GLUT1 in this study. Additionally, MafA has also been reported to increase mRNA levels of GCK, the rate-limiting enzyme for β-cell glucose metabolism (Wang and Iynedjian, 1997). In this study, GCK protein levels were differentially affected in MEHP exposure groups, increasing at low concentrations, and decreasing at high concentrations. In the MBP exposure groups, a decrease in GCK protein levels was observed in the high concentration group. These results suggest that while both MBP and MEHP affect PDX1 and MafA expression in 1.1B4 cells, they exhibit differences in their effects on other important factors such as insulin secretion, GLUT1 and GCK protein levels, highlighting the specificity of their effects on beta cell function and metabolic pathways. However, further studies are needed to fully elucidate the mechanisms underlying these different responses and to better elucidate the complex interplay between these chemicals and the intricate regulatory network of beta cell biology.

JNK, or c-Jun N-terminal kinase, is a stress-activated protein kinase that plays a role in cell response to various stressors, including oxidative stress and ER stress (Yung and Giacca, 2020). The decrease in JNK expression may indicate modulation of stress-related pathways, possibly as a protective response to counteract the adverse effects of chemical exposure. JNK expression decreased with 0.1, 10 and 1000 μM MEHP and 0.001 and 0.1 μM MBP. This observed reduction in JNK expression levels may be due to the effects of MEHP and MBP exposure on cellular signaling pathways. Activation of the ER stress pathway triggers GADD153 expression, which accelerates pancreatic beta cell destruction and has been implicated in the progression of diabetes (Lawrence et al., 2007). Disruption of the GADD153 gene delays the onset of ER stress-induced diabetes, highlighting its role in exacerbating the diabetic state. Studies have shown that inducing ER stress can reduce the expression of PPARγ in cells (Ryu et al., 2020). GADD153 is a transcription factor induced by endoplasmic reticulum stress and has been shown to bind to the PPARγ gene to inhibit PPARγ expression (Zhang et al., 2022). Furthermore, in ALF mice, an inverse relationship was observed between the gene and protein expression of GADD153 and PPARα. Activation of PPARα led to a reduction in GADD153 levels, while PPARα knockdown resulted in an increase in GADD153 expression (Zhang et al., 2017b). In this study, GADD153 expression levels increased in all MEHP and MBP exposure groups compared to the control group, except decreased in 1000 μM MEHP-treated cells. Additionally, this study revealed distinct responses in the expression levels of PPARα and PPARγ upon exposure to MEHP and MBP. In the MEHP-exposed groups, a concentration-dependent decrease in the expression of both PPARα and PPARγ was observed, except for PPARγ levels in the low-dose group. In contrast, the MBP exposure group showed a decrease in PPARα protein levels at all doses except the high dose, and a consistent decrease in PPARγ protein levels following exposure to MBP except for high dose group. These findings highlight the intricate regulatory responses of PPARα and PPARγ to MEHP and MBP exposure and underscore the complexity of phthalate-induced effects on pancreatic beta cell function. As in other studies, ER stress-mediated down-regulation of PPARα and PPARγ was observed in this study (Yuliana et al., 2019; Xu et al., 2020).

Recent research conducted both in vivo and in vitro indicates that the presence of phthalate metabolites leads to elevated production of pro-inflammatory cytokines (Zhou et al., 2019; Bølling et al., 2020). NF-κB is a key transcription factor that regulates inflammation and ER stress has the potential to induce activation of NF-κB (Kitamura, 2009). GADD153 modulation of PPARγ activity in human intestinal epithelial cells in response to ER stress leads to potentiation of proinflammatory NF-κB activation (Park et al., 2010). Intriguingly, NF-κB expression exhibited contrasting outcomes in 1.1B4 cells treated with MEHP and MBP in this study. Specifically, NF-κB expression levels decreased at a concentration of 1000 μM MEHP exposure and increased at 0.001 and 0.1 μM MEHP exposure, whereas MBP exposure resulted in increased expression compared to the control group. Remarkably, in cells treated with 1000 μM MBP, NF-κB expression levels nearly doubled. The significant upregulation of NF-κB in 1.1B4 cells exposed to MBP may indicate a more pronounced pro-inflammatory effect and warrants further investigation into the precise mechanisms by which these compounds influence NF-κB expression and its downstream effects. Exposure to MEHP and MBP resulted in reduced JNK expression at various concentrations, possibly indicating modulation of stress-related pathways as a protective response to chemical exposure (Yung and Giacca, 2020). The ER stress-induced GADD153 expression implicated in diabetes progression is consistent with the NF-κB expression differences observed in cells exposed to MEHP and MBP, suggesting complex molecular responses (Kitamura, 2009; Park et al., 2010). The different GADD153 expression patterns between exposures, coupled with the contrasting NF-κB results, highlight the complex interplay between ER stress, inflammation, and the effects of MEHP and MBP exposure.

It has been proposed that islet beta cell subpopulations include cells in a state of adaptation to ER stress (low levels of MafA and PDX1) and recovery from ER stress (high levels of MafA and PDX1) (Chen et al., 2022). In the present study, the high MafA and PDX1 protein expression levels observed in 1.1B4 pancreatic beta cells after 24 h exposure to MEHP and MBP may indicate recovery adaptation after ER stress. Nevertheless, it is noteworthy that the marked increase in lipid peroxidation, NF-κB protein expression and the moderate necrosis after MBP exposure observed, especially at the high dose, suggest that this adaptation is not sufficient for cell survival in this concentration group (1000 μM). In addition, the effects of prolonged exposure to MEHP and MBP on this recovery adaptation in 1.1B4 cells require further study. The doses used in this study cover concentrations at and below levels both relevant to human exposure and currently reported in environmental contexts (Morgenstern et al., 2017; Sakhi et al., 2017; Li et al., 2022; Liu et al., 2022; Peng et al., 2023; Wang et al., 2023). Overall, although both chemicals showed toxic effects on the 1.1B4 pancreatic beta cells, the data indicate that MEHP is more effective in inducing adverse outcomes on cell viability, proliferation, and stress response pathways than MBP. Given the increasing prevalence of diabetes worldwide, there is a growing need to further investigate the potential effects of such chemical exposures on pancreatic beta cells. Furthermore, it is of considerable importance that more extensive investigations are conducted to elucidate the lasting effects of long-term exposure to MEHP and MBP on the recovery adaptation of 1.1B4 cells.

CRediT authorship contribution statement

Fulya Dal Yöntem: Conceptualization, Methodology, Validation, Formal analysis, Data curation, Software, Writing – original draft. **Sinem Ayaz:** Investigation. **Şeyma Bulut:** Investigation. **Ebru Hacıosmanoğlu Aldoğan :** Investigation, Methodology, Writing – original draft. **Müfide Aydoğan Ahbab:** Conceptualization, Re-

CORRECTED PROOF

sources, Supervision, Validation, Writing – original draft. Writing – review & editing.

Declaration of Competing Interest

The authors declare that they have no known competing financial interests or personal relationships that could have appeared to influence the work reported in this paper.

Data Availability

Data will be made available on request.

Acknowledgements

This work was mainly supported by University of Health Sciences Türkiye, Scientific Research Coordination Unit (Project Number: 2021/024). This work was also partially funded by Scientific Research Projects Unit of Haliç University (Project Number: HBAP604-I-4).

References

ADA, 2014. Diagnosis and classification of diabetes mellitus. Diabetes Care 37 (1), S81–S90.
ADA, 2020. 2. Classification and diagnosis of diabetes: standards of medical care in diabetes—2021 American diabetes association. Diabetes Care S15–S33.
Armstrong, D., Browne, R., 1994. The analysis of free radicals, lipid peroxides, antioxidant enzymes and compounds related to oxidative stress as applied to the clinical chemistry laboratory. Adv. Exp. Med. Biol. 366, 43–58.
Bhandary, B., Marahatta, A., Kim, H.-R., Chae, H.-J., 2013. An involvement of oxidative stress in endoplasmic reticulum stress and its associated diseases. Int. J. Mol. Sci. 14, 434–456.
Bølling, A.K., Sripada, K., Becher, R., Bekö, G., 2020. Phthalate exposure and allergic diseases: Review of epidemiological and experimental evidence. Environ. Int. 139, 105706.
Boya, P., Kroemer, G., 2008. Lysosomal membrane permeabilization in cell death. Oncogene 27, 6434–6451.
Bräuner, E.V., Uldbjerg, C.S., Lim, Y.H., Gregersen, L.S., Krause, M., Frederiksen, H., Andersson, A.M., 2022. Presence of parabens, phenols and phthalates in paired maternal serum, urine and amniotic fluid. Environ. Int 158, 106987.
Cao, S.S., Kaufman, R.J., 2014. Endoplasmic reticulum stress and oxidative stress in cell fate decision and human disease. Antioxid. Redox Signal. 21, 396–413.
Cerf, M.E., 2013. Beta cell dysfunction and insulin resistance. Front. Endocrinol. 4, 37.
Chen, C.W., Guan, B.J., Alzahrani, M.R., Gao, Z., Gao, L., Bracey, S., Wu, J., Mbow, C.A., Jobava, R., Haataja, L., Zalavadia, A.H., Schaffer, A.E., Lee, H., LaFramboise, T., Bederman, I., Arvan, P., Mathews, C.E., Gerling, I.C., Kaestner, K.H., Tirosh, B., Engin, F., Hatzoglou, M., 2022. Adaptation to chronic ER stress enforces pancreatic β-cell plasticity. Nat. Commun. 13, 4621.
Dales, R.E., Kauri, L.M., Cakmak, S., 2018. The associations between phthalate exposure and insulin resistance, β-cell function and blood glucose control in a population-based sample. Sci. Total Environ. 612, 1287–1292.
Del Bubba, M., Ancillotti, C., Checchini, L., Fibbi, D., Rossini, D., Ciofi, L., Rivoira, L., Profeti, C., Orlandini, S., Furlanetto, S., 2018. Determination of phthalate diesters and monoesters in human milk and infant formula by fat extraction, size-exclusion chromatography clean-up and gas chromatography-mass spectrometry detection. J. Pharm. Biomed. Anal. 148, 6–16.
Deng, T., Zhang, Y., Wu, Y., Ma, P., Duan, J., Qin, W., Yang, X., Chen, M., 2018. Dibutyl phthalate exposure aggravates type 2 diabetes by disrupting the insulin-mediated PI3K/AKT signaling pathway. Toxicol. Lett. 290, 1–9.
Dong, R., Zhao, S., Zhang, H., Chen, J., Zhang, M., Wang, M., Wu, M., Li, S., Chen, B., 2017. Sex differences in the association of urinary concentrations of phthalates metabolites with self-reported diabetes and cardiovascular diseases in shanghai adults. Int. J. Environ. Res. Public Health 14.
Duan, Y., Wang, L., Han, L., Wang, B., Sun, H., Chen, L., Zhu, L., Luo, Y., 2017. Exposure to phthalates in patients with diabetes and its association with oxidative stress, adiponectin, and inflammatory cytokines. Environ. Int. 109, 53–63.
Eriksson, I., Vainikka, L., Persson, H.L., Öllinger, K., 2023. Real-time monitoring of lysosomal membrane permeabilization using acridine orange. Methods Protoc. 6, 72.
Fonseca, S.G., Gromada, J., Urano, F., 2011. Endoplasmic reticulum stress and pancreatic β-cell death. Trends Endocrinol. Metab. 22, 266–274.
Fujimoto, K., Polonsky, K.S., 2009. Pdx1 and other factors that regulate pancreatic beta-cell survival. Diabetes Obes. Metab. 11 (Suppl 4), 30–37.
Güven, C., Dal, F., Aydoğan Ahbab, M., Taskin, E., Ahbab, S., Adin Çinar, S., Sırma Ekmekçi, S., Güleç, Ç., Abacı, N., Akçakaya, H., 2016. Low dose monoethyl phthalate (MEP) exposure triggers proliferation by activating PDX-1 at 1.1B4 human pancreatic beta cells. Food Chem. Toxicol. 93, 41–50.
Hall, 1999. The role of glutathione in the regulation of apoptosis. Eur. J. Clin. Investig. 29, 238–245.
Hammel, S.C., Levasseur, J.L., Hoffman, K., Phillips, A.L., Lorenzo, A.M., Calafat, A.M., Webster, T.F., Stapleton, H.M., 2019. Children's exposure to phthalates and non-phthalate plasticizers in the home: The TESIE study. Environ. Int. 132, 105061.
Huang, T., Saxena, A.R., Isganaitis, E., James-Todd, T., 2014. Gender and racial/ethnic differences in the associations of urinary phthalate metabolites with markers of diabetes risk: National Health and Nutrition Examination Survey 2001-2008. Environ. Health 13, 6.
IDF, 2021. IDF Diabetes Atlas. I.D. Federation (Ed). Belgium, Brussels.
James-Todd, T.M., Meeker, J.D., Huang, T., Hauser, R., Ferguson, K.K., Rich-Edwards, J.W., McElrath, T.F., Seely, E.W., 2016. Pregnancy urinary phthalate metabolite concentrations and gestational diabetes risk factors. Environ. Int. 96, 118–126.
Karabulut, G., Barlas, N., 2021. The possible effects of mono butyl phthalate (MBP) and mono (2-ethylhexyl) phthalate (MEHP) on INS-1 pancreatic beta cells. Toxicol. Res. 10, 601–612.
Katerji, M., Filippova, M., Duerksen-Hughes, P., 2019. Approaches and methods to measure oxidative stress in clinical samples: research applications in the cancer field. Oxid. Med. Cell. Longev. 2019. 1279250-1279250.
Kitamura, M., 2009. Biphasic, bidirectional regulation of NF-kappaB by endoplasmic reticulum stress. Antioxid. Redox Signal 11, 2353–2364.
Kitamura, Y.I., Kitamura, T., Kruse, J.P., Raum, J.C., Stein, R., Gu, W., Accili, D., 2005. FoxO1 protects against pancreatic beta cell failure through NeuroD and MafA induction. Cell Metab. 2, 153–163.
Latini, G., 2005. Monitoring phthalate exposure in humans. Clin. Chim. Acta 361, 20–29.
Li, A.J., Martinez-Moral, M.-P., Al-Malki, A.L., Al-Ghamdi, M.A., Al-Bazi, M.M., Kumosani, T.A., Kannan, K., 2019. Mediation analysis for the relationship between urinary phthalate metabolites and type 2 diabetes via oxidative stress in a population in Jeddah, Saudi Arabia. Environ. Int. 126, 153–161.
Li, Z., Wu, D., Guo, Y., Mao, W., Zhao, N., Zhao, M., Jin, H., 2022. Phthalate metabolites in paired human serum and whole blood. Sci. Total Environ. 824, 153792.
Lin, Y., Wei, J., Li, Y., Chen, J., Zhou, Z., Song, L., Wei, Z., Lv, Z., Chen, X., Xia, W., Xu, S., 2011. Developmental exposure to di(2-ethylhexyl) phthalate impairs endocrine pancreas and leads to long-term adverse effects on glucose homeostasis in the rat. Am. J. Physiol. -Endocrinol. Metab. 301, E527–E538.
Liu, M., Zhao, L., Liu, L., Guo, W., Yang, H., Chen, S., Yu, J., Li, M., Fang, Q., Lai, X., Yang, L., Zhu, R., Zhang, X., 2022. Urinary phthalate metabolites mixture, serum cytokines and renal function in children: a panel study. J. Hazard. Mater. 422, 126963.
Lu, M., Gong, X., 2009. Upstream reactive oxidative species (ROS) signals in exogenous oxidative stress-induced mitochondrial dysfunction. Cell Biol. Int. 33, 658–664.
Lushchak, V.I., 2014. Free radicals, reactive oxygen species, oxidative stress and its classification. Chem. Biol. Inter. 224, 164–175.
Mangala Priya, V., Mayilvanan, C., Akilavalli, N., Rajesh, P., Balasubramanian, K., 2014. Lactational exposure of phthalate impairs insulin signaling in the cardiac muscle of F1 female albino rats. Cardiovasc. Toxicol. 14, 10–20.
Martinelli, M.I., Mocchiutti, N.O., Bernal, C.A., 2006. Dietary di(2-ethylhexyl)phthalate-impaired glucose metabolism in experimental animals. Hum. Exp. Toxicol. 25, 531–538.
McCluskey, J.T., Hamid, M., Guo-Parke, H., McClenaghan, N.H., Gomis, R., Flatt, P.R., 2011. Development and Functional Characterization of Insulin-releasing Human Pancreatic Beta Cell Lines Produced by Electrofusion*. J. Biol. Chem. 286, 21982–21992.
McCulloch, L.J., van de Bunt, M., Braun, M., Frayn, K.N., Clark, A., Gloyn, A.L., 2011. GLUT2 (SLC2A2) is not the principal glucose transporter in human pancreatic beta cells: implications for understanding genetic association signals at this locus. Mol. Genet. Metab. 104, 648–653.
Mok, S., Lim, J.-E., Lee, A., Kim, S., Kim, S., Lee, I., Kho, Y., Park, J., Kim, S., Choi, K., Moon, H.-B., 2022. Within- and between-person variability of urinary phthalate metabolites and bisphenol analogues over seven days: considerations of biomonitoring study design. Environ. Res. 209, 112885.
Moreau, M., Mallick, P., Smeltz, M., Haider, S., Nicolas, C.I., Pendse, S.N., Leonard, J.A., Linakis, M.W., McMullen, P.D., Clewell, R.A., Clewell, H.J., Yoon, M., 2022. Considerations for improving metabolism predictions for in vitro to in vivo extrapolation. Front. Toxicol. 4, 894569.
Morgenstern, R., Whyatt, R.M., Insel, B.J., Calafat, A.M., Liu, X., Rauh, V.A., Herbstman, J., Bradwin, G., Factor-Litvak, P., 2017. Phthalates and thyroid function in preschool age children: sex specific associations. Environ. Int. 106, 11–18.
Nam, D.J., Kim, Y., Yang, E.H., Lee, H.C., Ryoo, J.-H., 2020. Relationship between urinary phthalate metabolites and diabetes: Korean National Environmental Health Survey (KoNEHS) cycle 3 (2015-2017). Ann. Occup. Environ. Med. 32. . e34-e34.
Nasteska, D., Fine, N.H.F., Ashford, F.B., Cuozzo, F., Viloria, K., Smith, G., Dahir, A., Dawson, P.W.J., Lai, Y.C., Bastidas-Ponce, A., Bakhti, M., Rutter, G.A., Fiancette, R., Nano, R., Piemonti, L., Lickert, H., Zhou, Q., Akerman, I., Hodson, D.J., 2021. PDX1 (LOW) MAFA(LOW) β-cells contribute to islet function and insulin release. Nat. Commun. 12, 674.
Net, S., Sempéré, R., Delmont, A., Paluselli, A., Ouddane, B., 2015. Occurrence, fate, behavior and ecotoxicological state of phthalates in different environmental matrices. Environ. Sci. Technol. 49, 4019–4035.
Park, S.H., Choi, H.J., Yang, H., Do, K.H., Kim, J., Lee, D.W., Moon, Y., 2010. Endoplasmic reticulum stress-activated C/EBP homologous protein enhances nuclear factor-kappaB signals via repression of peroxisome proliferator-activated receptor gamma. J. Biol. Chem. 285, 35330–35339.
Peng, M.Q., Karvonen-Gutierrez, C.A., Herman, W.H., Mukherjee, B., Park, S.K., 2023. Phthalates and Incident Diabetes in Midlife Women: The Study of Women's Health Across the Nation (SWAN). J. Clin. Endocrinol. Metab. 108, 1947–1957.
Rajesh, P., Sathish, S., Srinivasan, C., Selvaraj, J., Balasubramanian, K., 2013. Phthalate is associated with insulin resistance in adipose tissue of male rat: role of antioxidant vitamins. J. Cell. Biochem. 114, 558–569.
Ryu, K.-Y., Jeon, E.J., Leem, J., Park, J.-H., Cho, H., 2020. Regulation of adipsin

UNCORRECTED PROOF

expression by endoplasmic reticulum stress in adipocytes. Biomolecules 10, 314.
Saengkaew, T., Jantarat, C., Nosoognoen, W., Supornsilchai, V., 2017. Association between urinary phthalates and metabolic abnormalities in obese Thai children and adolescents. J. Pediatr. Endocrinol. Metab. 30, 931–938.
Sakhi, A.K., Sabaredzovic, A., Cequier, E., Thomsen, C., 2017. Phthalate metabolites in Norwegian mothers and children: Levels, diurnal variation and use of personal care products. Sci. Total Environ. 599–600, 1984–1992.
Sano, R., Reed, J.C., 2013. ER stress-induced cell death mechanisms. Biochim. Biophys. Acta 1833, 3460–3470.
Serrano-Puebla, A., Boya, P., 2016. Lysosomal membrane permeabilization in cell death: new evidence and implications for health and disease. Ann. N. Y. Acad. Sci. 1371, 30–44.
She, Y., Jiang, L., Zheng, L., Zuo, H., Chen, M., Sun, X., Li, Q., Geng, C., Yang, G., Jiang, L., Liu, X., 2017. The role of oxidative stress in DNA damage in pancreatic β cells induced by di-(2-ethylhexyl) phthalate. Chem. Biol. Interact. 265, 8–15.
Shi, L., Jiang, L., Zhang, X., Yang, G., Zhang, C., Yao, X., Wu, X., Fu, M., Sun, X., Liu, X., 2020. Pyrroloquinoline quinone protected autophagy-dependent apoptosis induced by mono(2-ethylhexyl) phthalate in INS-1 cells. Hum. Exp. Toxicol. 39, 194–211.
Stael, S., Miller, L.P., Fernandez-Fernandez, A.D., Van Breusegem, F., 2022. Detection of damage-activated metacaspase activity by western blot in plants. Methods Mol. Biol. 2447, 127–137.
Sun, H., Zhang, A., Gong, Y., Sun, W., Yan, B., Lei, S., Yao, L.-H., 2022. Improving effect of cordycepin on insulin synthesis and secretion in normal and oxidative-damaged INS-1 cells. Eur. J. Pharmacol. 920, 174843.
Sun, X., Lin, Y., Huang, Q., Shi, J., Qiu, L., Kang, M., Chen, Y., Fang, C., Ye, T., Dong, S., 2015. Di(2-ethylhexyl) phthalate-induced apoptosis in rat INS-1 cells is dependent on activation of endoplasmic reticulum stress and suppression of antioxidant protection. J. Cell. Mol. Med. 19, 581–594.
Venturelli, A.C., Meyer, K.B., Fischer, S.V., Kita, D.H., Philipsen, R.A., Morais, R.N., Martino Andrade, A.J., 2019. Effects of in utero and lactational exposure to phthalates on reproductive development and glycemic homeostasis in rats. Toxicology 421, 30–40.
Wang, F., Gómez-Sintes, R., Boya, P., 2018. Lysosomal membrane permeabilization and cell death. Traffic 19, 918–931.
Wang, H., Brun, T., Kataoka, K., Sharma, A.J., Wollheim, C.B., 2007. MAFA controls genes implicated in insulin biosynthesis and secretion. Diabetologia 50, 348–358.
Wang, H., Chen, R., Gao, Y., Qu, J., Zhang, Y., Jin, H., Zhao, M., Bai, X., 2023. Serum concentrations of phthalate metabolites in pregnant women and their association with gestational diabetes mellitus and blood glucose levels. Sci. Total Environ. 857, 159570.
Wang, H., Iynedjian, P.B., 1997. Modulation of glucose responsiveness of insulinoma beta-cells by graded overexpression of glucokinase. Proc. Natl. Acad. Sci. USA 94, 4372–4377.
Wang, Y., Zhu, H., Kannan, K., 2019. A review of biomonitoring of phthalate exposures. Toxics 7, 21.
Weldingh, N.M., Jørgensen-Kaur, L., Becher, R., Holme, J.A., Bodin, J., Nygaard, U.C., Bølling, A.K., 2017. Bisphenol A is more potent than phthalate metabolites in reducing pancreatic β-cell function. Biomed. Res. Int. 2017, 4614379.
Wu, G., Fang, Y.Z., Yang, S., Lupton, J.R., Turner, N.D., 2004. Glutathione metabolism and its implications for health. J. Nutr. 134, 489–492.
Wu, X., Jiang, L., Sun, X., Yao, X., Bai, Y., Liu, X., Liu, N., Zhai, X., Wang, S., Yang, G., 2017. Mono(2-ethylhexyl) phthalate induces autophagy-dependent apoptosis through lysosomal-mitochondrial axis in human endothelial cells. Food Chem. Toxicol. 106, 273–282.
Xu, L., Zhang, X., Tian, Y., Fan, Z., Li, W., Liu, M., Hu, J., Duan, Z., Jin, R., Ren, F., 2020. The critical role of PPARα in the binary switch between life and death induced by endoplasmic reticulum stress. Cell Death Dis. 11, 691.
Yuliana, A., Daijo, A., Jheng, H.-F., Kwon, J., Nomura, W., Takahashi, H., Ara, T., Kawada, T., Goto, T., 2019. Endoplasmic reticulum stress impaired uncoupling protein 1 expression via the suppression of peroxisome proliferator-activated receptor γ binding activity in mice beige adipocytes. Int. J. Mol. Sci. 20, 274.
Yung, J.H.M., Giacca, A., 2020. Role of c-Jun N-terminal kinase (JNK) in obesity and type 2 diabetes. Cells 9, 706.
Zhang, W., Shen, Xy, Zhang, W.-w, Chen, H., Xu, W.-p, Wei, W., 2017a. Di-(2-ethylhexyl) phthalate could disrupt the insulin signaling pathway in liver of SD rats and L02 cells via PPARγ. Toxicol. Appl. Pharmacol. 316, 17–26.
Zhang, X., Dong, P., Shi, H., Sun, H., Lin, J., Chen, D., Duan, Z., Li, X., Ren, F., 2017b. Peroxisome proliferator-activated receptor alpha mediates C/EBP homologous protein to protect mice from acute liver failure. Inflamm. Res. 66, 813–822.
Zhang, X., Jiang, L., Chen, H., Wei, S., Yao, K., Sun, X., Yang, G., Jiang, L., Zhang, C., Wang, N., Wang, Y., Liu, X., 2022. Resveratrol protected acrolein-induced ferroptosis and insulin secretion dysfunction via ER-stress- related PERK pathway in MIN6 cells. Toxicology 465, 153048.
Zhou, L., Chen, H., Xu, Q., Han, X., Zhao, Y., Song, X., Zhao, T., Ye, L., 2019. The effect of di-2-ethylhexyl phthalate on inflammation and lipid metabolic disorder in rats. Ecotoxicol. Environ. Saf. 170, 391–398.

CORRECTED PROOF